

10

74022

GEMP-640

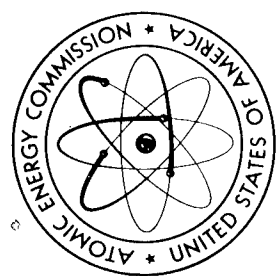
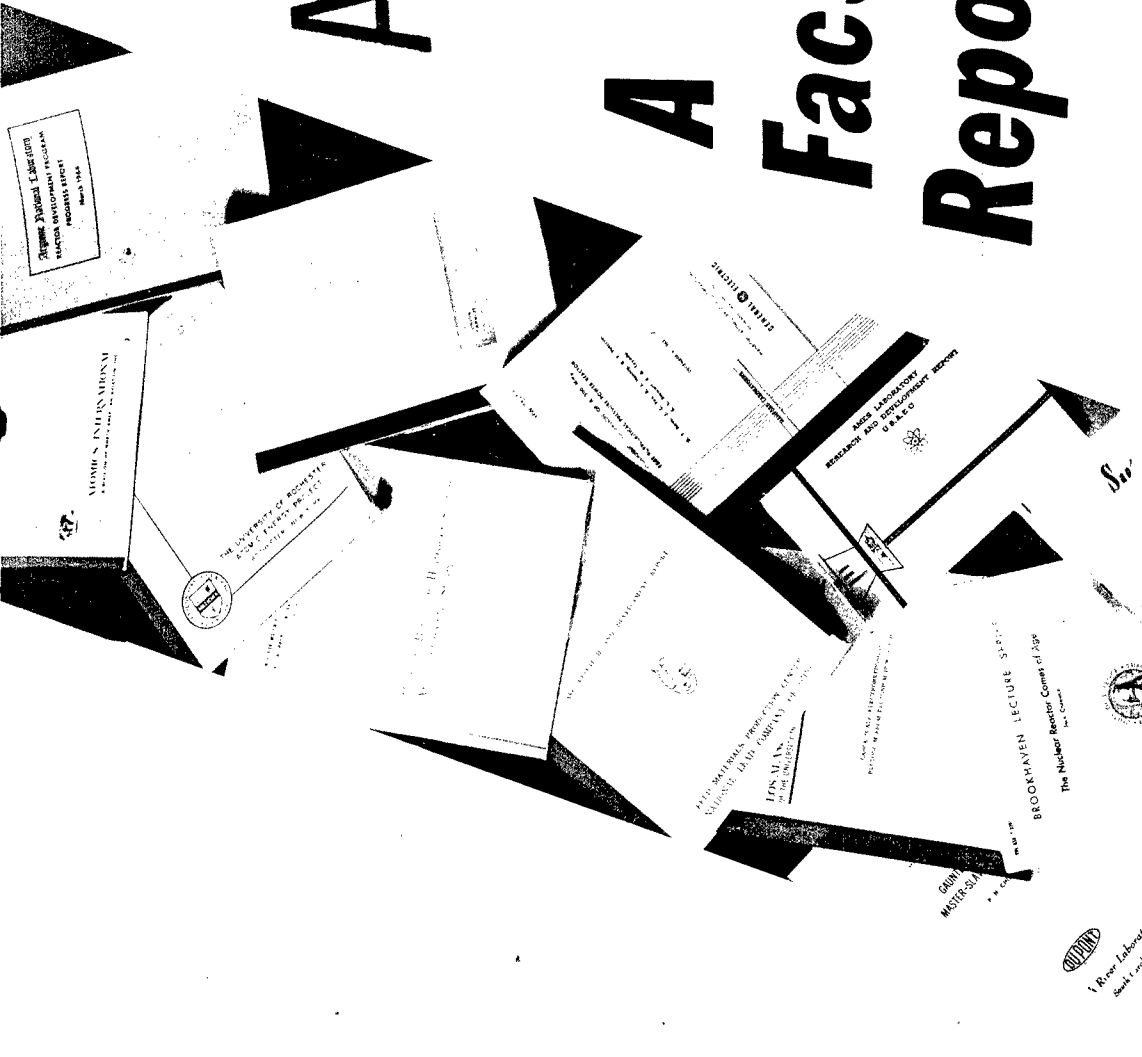
# AMPTIAC

# A Facsimile Report

Reproduced by  
**UNITED STATES**  
**ATOMIC ENERGY COMMISSION**  
 Division of Technical Information  
 P.O. Box 62 Oak Ridge, Tennessee 37830

Reproduced From  
 Best Available Copy

100% QUALITY INSPECTED 4

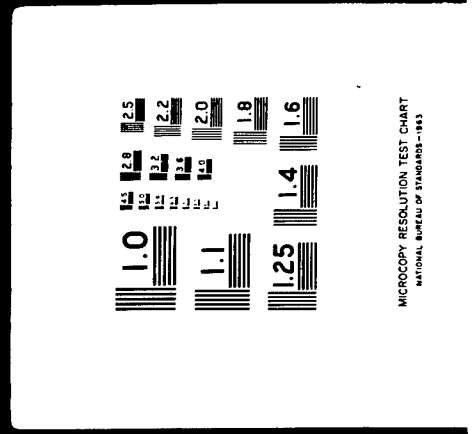


# 20000908 227

I 'OF I

GEMP

640





### INTRODUCTION

The need for structural materials capable of operating at ultra-high temperatures has focused attention on the refractory metals and alloys. Of particular interest are the high temperature creep properties of these metals. In a recent replica electron microscopy investigation of the creep deformation of tungsten, Stiegler, et al.<sup>(1)</sup> studied the formation of voids or cavities at the grain boundaries of powder metallurgy processed material creep-rupture tested at 1650°C and 2200°C. They found that at both test temperatures their specimens generally failed in a brittle manner, and they attributed this failure to the growth and linking up of grain boundary cavities.

Recently, however, it has been shown that while powder metallurgy tungsten creep-rupture tested at temperatures ranging from 1600° to 3000°C failed in a brittle, intergranular manner, specimens prepared from arc-cast material and tested under similar conditions failed in a ductile manner.<sup>(2)</sup> Likewise, high temperature stress-rupture tests of molybdenum have shown similar differences in the failure behavior of powder metallurgy and arc-cast material.<sup>(3)</sup> These results indicate that different mechanisms of failure are operating in the two types of materials. In an attempt to determine this basic difference, an optical microscopy and electron fractography study of creep-rupture tested powder metallurgy and arc-cast tungsten was undertaken.

### EXPERIMENTAL TECHNIQUES

The studies were carried out on six powder metallurgy and four arc-cast tungsten specimens selected from groups tested and reported by Flagella.<sup>(2)</sup> These specimens were made from rolled and stress-relieved sheet, with the thicknesses being 0.5 mm for powder metallurgy specimens and 1.5 mm for arc-cast specimens. Both groups of specimens had 25.4 mm gage lengths and 6.4 mm gage widths. [Chemical analyses of fabricated test samples indicated interstitial impurity contents of 28 ppm C, 10 ppm O, 2 ppm H, and 0.8 ppm N for the powder metallurgy material, and 63 ppm C, 5.6 ppm O, 0.7 ppm H, and 0.1 ppm N for the arc-cast material.] Substitutional impurity levels were below detectable limits for both materials. [Specimens examined had been creep-rupture tested at 1600°, 2000°, 2200°, and 2600°C, with the results listed in Table 1.]

For the fractographic study, fresh fracture surfaces in the highly stressed region near the original break were created by clamping the specimen in a vise, allowing about 3 mm of the broken end to protrude, and sharply rapping the protruding end. These newly exposed surfaces were then replicated by the standard two-stage plastic/carbon technique, using chromium shadowing, and examined in the electron microscope. ] → P.S

After replication, these same pieces were mounted and mechanically polished for metallographic examination. The pieces were mounted edge-on, with the view perpendicular to the stress axis, and were examined and photographed in the as-polished condition. In this way, any stress-induced porosity was observed in its original state, unaltered by chemical attack. Following examination for porosity, some of the specimens were etched for grain size evaluation.

## RESULTS

Optical microscopy of the as-polished surfaces showed an abundance of grain boundary cavities in the powder metallurgy tungsten, and an almost total lack of such cavities in the arc-cast material. Representative micrographs are presented in Fig. 1, where Figs. 1(a) and (b) refer to powder metallurgy material, and Figs. 1(c) and (d) refer to arc-cast material.

As illustrated by these micrographs, the powder metallurgy material consisted of fairly equiaxed grains, which increased in average size with increasing test temperature. Grain boundary separation and cavitation were very pronounced, especially along boundaries which were transverse to the stress direction. On the other hand, arc-cast material was composed of very large grains, which extended across the total thickness of the specimens, and showed practically no tendency to form cavities. A rare instance of a grain boundary cavity in the arc-cast specimen tested at 1600°C is arrowed in Fig. 1(c).

Replica electron microscopy of the powder metallurgy samples showed that the mode of fracture was almost totally intergranular, especially for the lower temperature, higher stress conditions, and that the exposed grain boundary surfaces contained a profusion of cavities. Typical examples are illustrated in Fig. 2. At lower temperatures the voids were usually irregular in shape, tending to be relatively flattened along the boundary surface and often containing elongated "fingers", suggestive of void coalescence, Fig. 2(a). Such cavities are termed wedge-shaped, or w-type (4), and are believed to originate primarily by grain boundary

sliding. (5,6) At higher temperatures the shape of the cavities became more polyhedral, especially after lower stress, longer time tests, Fig. 2(b). These more rounded, or r-type (4) voids, are bounded by flat crystallographic facets which correspond to low-index planes of the cubic lattice. (7) Such polyhedral voids form under conditions where surface diffusion allows the cavities to reduce their surface tension and assume equilibrium shapes. Although a few examples were seen of creep cavities aligned along grain boundary triple junctions, Fig. 2(c), there was nothing to indicate that such junctions were preferred sites for voids. In general, both w-type and r-type cavities tended to be distributed uniformly over the grain boundary surfaces, in agreement with the observations of Stiegler, et al. (1)

In contrast to the powder metallurgy material, replica electron micrographs of the arc-cast tungsten showed that the fracture at all temperatures was predominantly transgranular, as illustrated in Fig. 3(a). When grain boundary surfaces were seen, they were always relatively clean and contained only a few small irregularities suggestive of cavities, Fig. 3(b). In none of these samples was any evidence seen of cavity coalescence or polyhedral shaped voids.

An attempt was made to quantitatively correlate the observed microstructural features with the mechanical properties of the creep tested specimens. This involved measurements of the open porosity and grain size in the powder metallurgy specimens, with the results listed in Table I. However, meaningful measurements could not be made on the arc-cast material because of the lack of porosity and the extremely large grain size.

For the powder metallurgy tungsten, which failed with relatively little elongation in comparison with the arc-cast material, it was of interest to determine whether all of that elongation was caused by cavitation, or whether other mechanisms also contributed. Accordingly, lineal measurements of open porosity were made from the as-polished surfaces at 250X magnification. These measurements were made parallel to the stress (elongation) direction at a distance of approximately 3-4 mm from the original fracture of each specimen, in regions similar to those shown in Figs. 1(a) and (b). The averages of ten measurements made on each sample were converted to percentages of the length sampled, and are listed in column 8 of Table 1.

Maximum possible void content in the stress direction, assuming that the total elongation was due to cavitation, was calculated from the measured elongations listed in column 6 of Table 1, using the relation:

$$\text{max. void content (\%)} = \frac{\text{elongation (\%)} \times 100}{100 + \text{elongation (\%)}}$$

Comparison of these values, listed in column 7 of the table, with the measured values of column 8 shows that only a portion of the total elongation can be accounted for by the cavities. However, this relative proportion remains essentially constant as the test temperature increases and overall ductility decreases. As shown in column 9 of the table, the portion of the elongation due to cavities is about 16% of that expected if cavitation were the only source of deformation.

To determine whether grain deformation had occurred during creep, lineal grain size measurements were made in the longitudinal (stress

and transverse directions, both in the high stress regions where creep cavity measurements had been made, and in the unstressed holder ends of the specimens. These measurements showed that in all specimens the grains were elongated approximately 40% in the stress direction, but that this elongation was the same in unstressed regions as in highly stressed regions. This elongation is undoubtedly the result of prior fabrication history, since the specimens were formed with their lengths parallel to the rolling direction of the starting sheet material. The lack of measureable grain deformation during creep indicates that part of the bulk deformation must, therefore, be due to grain boundary sliding.

#### DISCUSSION

Although these observations illustrate the pronounced difference in failure mechanisms of powder metallurgy and arc-cast tungsten, they do not indicate the underlying cause of this difference. Grain boundary failure, such as that observed in the powder metallurgy material, can occur if the matrix is strengthened without a corresponding strengthening of the boundaries, or if the boundaries themselves are weakened. Matrix hardening can be produced by a dispersion of impurities or precipitates, while grain boundary weakening can occur with preferential precipitation in the boundaries, especially if a continuous film of precipitate forms. By the same reasoning, transgranular fracture, such as that observed in the arc-cast tungsten, will be favored if the grain boundaries are strengthened with respect to the matrix. Such strengthening can arise through a decrease in the amount of segregated impurities at grain boundaries, thus leading to increased grain boundary mobility

and ductility. Alternatively, certain types of discontinuous precipitation at grain boundaries can strengthen those boundaries by blocking dislocation movement and preventing sliding.

In the optical and replica electron micrographs, no direct evidence was observed of precipitation either within the matrix or along grain boundaries. However, these techniques would not be expected to resolve very small precipitates. Therefore, a cursory transmission electron microscopy examination was made of thin foils prepared from both stressed and unstressed regions of several of the specimens included in this study.

These examinations likewise failed to show any precipitates in either of the two tungsten materials; however, small spherical pores were occasionally seen in the powder metallurgy material. This porosity occurred in both stressed and unstressed regions, and was not particularly associated with grain boundaries. These pores were concluded to be sintering pores, and may contribute to the brittle behavior of this material by impeding dislocation motion and by inhibiting grain boundary migration and grain growth.

#### SUMMARY

Optical and replica electron microscopy have been used to characterize the modes of creep failure in high purity arc-cast and powder metallurgy tungsten. The results may be summarized as follows:

1. Arc-cast tungsten fails in a ductile manner and fractures transgranularly, while powder metallurgy tungsten fails in a relatively brittle fashion and fractures intergranularly by the growth and link-up of creep cavities.

2. Creep cavities in powder metallurgy tungsten are irregular in shape and tend to be flattened along the grain boundaries at temperatures below about 2000°C, while at higher temperatures they take on polyhedral shapes bounded by crystallographic facets.

3. No microstructural evidence of precipitation was found to explain the basic difference in failure mechanisms of the two tungsten materials, but sintering pores present in the powder metallurgy tungsten are believed to contribute to its embrittlement.

#### ACKNOWLEDGEMENTS

The writers are grateful to P. N. Flagella and S. F. Bartram for helpful discussions during the course of this work.

## REFERENCES

1. J. O. Stiegler, K. Farrell, B. T. M. Loh, and H. E. McCoy, Trans. ASM 60 (1967) 494.
2. P. N. Flagella, "High Temperature Creep-Rupture Behavior of Unalloyed Tungsten", Third International Symposium, High Temperature Technology, Stanford Research Institute, Astilomar, Calif., Sept. 1967. To be published in Proceedings.
3. P. N. Flagella, AIAA Journal 5 (1967) 281.
4. F. Garofalo, Fundamentals of Creep and Creep-Rupture in Metals, Macmillan Series in Materials Science, New York, 1965, p. 213.
5. C. Zener, Elasticity and Anelasticity of Metals, University of Chicago Press, Chicago, 1948, p. 158.
6. H. C. Chang and N. J. Grant, Trans. AIME 206 (1956) 544.
7. K. Farrell, B. T. M. Loh, and J. O. Stiegler, Trans. ASM 60 (1967) 485.

Table 1. Tungsten Specimens Used for Study of Fatigue Mechanism

Sample Number	Test Temp., °C.	Stress		Time to Rupture, Hours	Elongation, %	Maximum Void Content, %	Measured Void Content, %	Ratio, Meas. Max. %	Average Grain Size, Microns
		kg/mm <sup>2</sup>	PSI						
POWDER METALLURGY									
W(4)-1-73									
1600	1600	4.22	6000	51.27	32	24.2	5.58	23.1	32.5
-79	2000	2.11	3000	23.17	27	21.3	2.46	11.5	38.0
-18	2200	1.41	2000	15.29	15	13.0	2.02	15.5	48.5
-10	2200	1.12	1600	60.65	17	14.5	2.11	14.6	48.5
-8	2600	0.84	1200	8.84	8	7.4	1.11	15.0	215.5
-7	2600	0.70	1000	25.08	5	4.8	0.90	18.8	264.0
ARC-CAST									
W(3)-48									
1600	1600	4.22	6000	30.90	76				
-53	2000	2.11	3000	6.70	70				
-14	2200	1.05	1500	40.70	106				
-25	2600	0.56	800	4.77	64				

Figure Captions

Figure 1. Optical micrographs of creep-rupture tested tungsten in as-polished condition. (a) Powder metallurgy specimen tested at 1600°C and 4.22 kg/mm<sup>2</sup>. (b) Powder metallurgy specimen tested at 2000°C and 2.11 kg/mm<sup>2</sup>. (c) Arc-cast specimen tested at 1600°C and 4.22 kg/mm<sup>2</sup>. (d) Arc-cast specimen tested at 2000°C and 2.11 kg/mm<sup>2</sup>.

Figure 2. Electron fractographs of powder metallurgy tungsten. (a) Irregular creep cavities in specimen tested at 1600°C and 4.22 kg/mm<sup>2</sup>. (b) Polyhedra shaped voids in specimen tested at 2600°C and 0.70 kg/mm<sup>2</sup>. (c) Cavities along a grain boundary triple junction in specimen tested at 2600°C and 0.84 kg/mm<sup>2</sup>.

Figure 3. Electron fractographs of arc-cast tungsten. (a) Transgranular fracture in specimen tested at 2000°C and 2.11 kg/mm<sup>2</sup>. (b) Grain boundary surface in specimen tested at 1600°C and 4.22 kg/mm<sup>2</sup>.

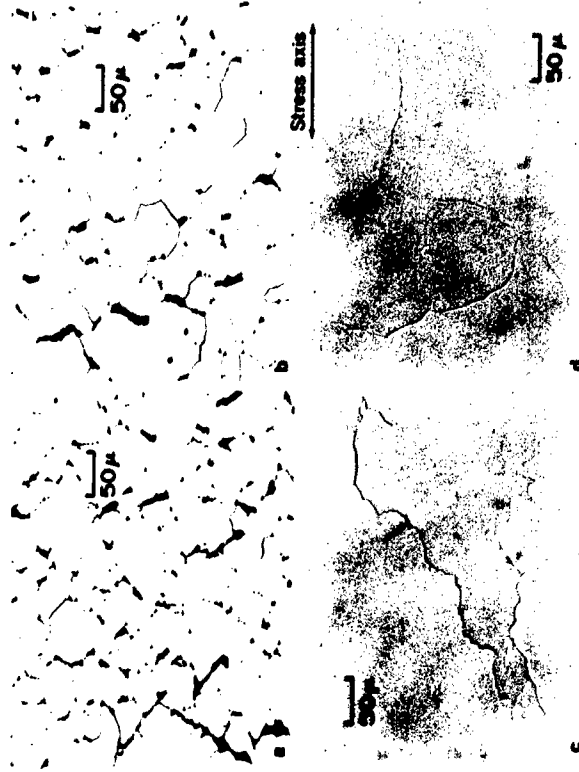


Figure 1. Optical micrographs of creep-rupture tested tungsten in as-polished condition. (a) Powder metallurgy specimen tested at 1600°C and 4.22 kg/mm<sup>2</sup>. (b) Powder metallurgy specimen tested at 2000°C and 2.11 kg/mm<sup>2</sup>. (c) Arc-cast specimen tested at 1600°C and 4.22 kg/mm<sup>2</sup>. (d) Arc-cast specimen tested at 2000°C and 2.11 kg/mm<sup>2</sup>.

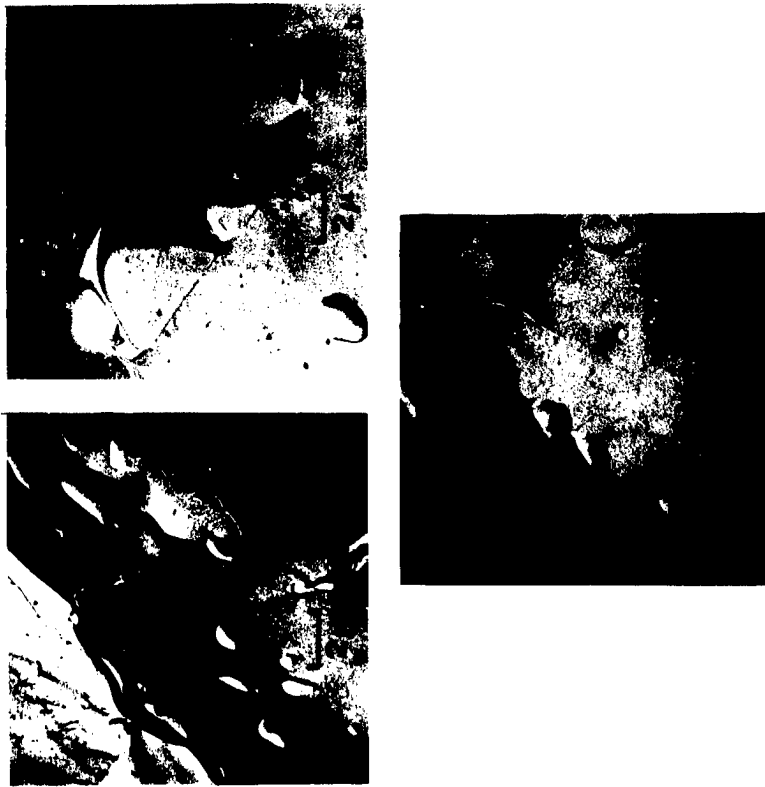


Figure 2. Electron fractographs of powder metallurgy tungsten. (a) Irregular creep cavities in specimen tested at 1600°C and 4.22 kg/mm<sup>2</sup>. (b) Polyhedral shaped voids in specimen tested at 2600°C and 0.70 kg/mm<sup>2</sup>. (c) Cavities along a grain boundary triple junction in specimen tested at 2600°C and 0.84 kg/mm<sup>2</sup>.



Figure 3. Electron fractographs of arc-cast tungsten. (a) Transgranular fracture in specimen tested at 2000°C and 2.11 kg/mm<sup>2</sup>. (b) Grain boundary surface in specimen tested at 1600°C and 4.22 kg/mm<sup>2</sup>.

**END**

**DATE FILMED**

**1 / 22 / 69**

*1.7 am*

 **KAROLTON KLASP®**  
**NO. 15 4 X 6 1/2**  
**KAROLTON ENVELOPE**  
**WEST CARROLLTON, OHIO**